

Vibrational line shapes of low-frequency adsorbate modes: CO on Pt(111)

B. N. J. Persson

Institut für Festkörperforschung, Kernforschungsanlage Jülich, D-5170 Jülich, Federal Republic of Germany

R. Ryberg

Department of Physics, Chalmers University of Technology, S-412 96 Gothenburg, Sweden

(Received 1 May 1989)

We present a study of the coverage and temperature dependence of the Pt-CO stretch vibration. As a function of coverage, the width of the absorption peak exhibits local minima at the ordered (4×4), (8×8), and $c(4 \times 2)$ structures. For the $c(4 \times 2)$ structure the temperature dependence of the peak width and position is in good agreement with the exchange model of vibrational phase relaxation. The exchange mode is found to be the parallel frustrated translation, i.e., the same mode that gives the dominating dephasing contribution to the C-O stretch vibration. For $T > 250$ K, the linewidth increases much stronger than predicted by the exchange model which is attributed to a thermally induced order-disorder transition. Finally, we present Monte Carlo simulations as a function of coverage, in order to study some aspects of the disorder-induced contributions to the linewidth.

I. INTRODUCTION

Infrared spectroscopy (IRS) has developed into a major surface-science technique.¹⁻⁴ The high sensitivity and the inherent high resolution is now also combined with a large spectral range ($400-4000 \text{ cm}^{-1}$). The high resolution allows fine details in the vibrational spectra to be resolved. In particular, the dependence of the vibrational line shape on the temperature and coverage contains very useful information which reflects the nature of the adsorbate-adsorbate and adsorbate-substrate interactions.

The origin of the line shape of the high-frequency C-O stretch vibration for CO adsorbed on metal surfaces is now well understood:⁴ at low temperature the linewidth is dominated by vibrational damping via excitation of electron-hole pairs giving rise to a temperature-independent contribution of $\sim 5 \text{ cm}^{-1}$. Superimposed on this is a temperature-dependent contribution which depends strongly on the metal substrate and on the binding site. This latter contribution is due to vibrational phase relaxation caused by anharmonic coupling between the C-O stretch vibration and low-frequency frustrated translations and rotations. For the C-O stretch vibration disorder-induced broadening is usually rather small owing to line narrowing caused by the strong-dipole-dipole coupling. On the other hand, for the CO-metal stretch vibration the dipole-dipole coupling is 2 orders of magnitude weaker and negligible line narrowing occurs as a result of this interaction. Hence it is not surprising to find that the CO-metal vibration is strongly dependent on the degree of order in the adsorbate system. In fact, the linewidth values presented in this work for CO on Pt(111) are smaller than those reported earlier by Tobin and Richards,⁵ by Hoge *et al.*,⁶ and by Malik and Trenary.⁷ We attribute this discrepancy to variations in the surface-preparation and adsorbate-deposition techniques.

In this work we present a detailed study of the temper-

ature and coverage dependence of the Pt-CO stretch vibration for the on-top bonded CO molecules chemisorbed on Pt(111). We find that as a function of coverage the linewidth exhibits local minima at the ordered structures. For the $c(4 \times 2)$ structure the temperature dependence of the peak width and position is in good agreement with the exchange model of vibrational phase relaxation. The exchange mode is found to be the parallel frustrated translation,⁸ i.e., the same mode that gives the dominating dephasing contribution to the C-O stretch vibration.⁹ For $T > 250$ K, the linewidth increases much stronger than predicted by the exchange model which is attributed to a thermally induced order-disorder transition. Finally, we present Monte Carlo (MC) simulations¹⁰ as a function of coverage, in order to study some aspects of the disorder-induced contribution to the linewidth.

This paper is organized as follows. In Sec. II we review and expand on the basic theoretical notion necessary for the interpretation of the experimental data. In particular we show that the direct metal-CO coupling gives a negligible contribution to the energy relaxation (multiple-phonon emission) and dephasing of the metal-CO vibrational mode and of most other low-frequency adsorbate modes. This result differs completely from the prevailing opinion¹¹⁻¹⁵ that this process can be a very important vibrational energy and phase relaxation process, but follows directly when accounting for an important factor which has been overlooked in all earlier work. We therefore believe that excitation of electron-hole pairs is the dominating *energy relaxation channel* for the metal-CO vibrational mode, and the dominating *dephasing contribution* is found to arise from anharmonic coupling between the Pt-C-O stretch vibration and the parallel frustrated translation, just as for the C-O stretch vibration. In Sec. III we outline the experimental procedure and present the experimental results. An analysis of the experimental data, based on the theoretical materi-

al presented in Sec. II and also on Monte Carlo simulations, is presented in Sec. IV. The Monte Carlo simulations have been performed as a function of CO coverage in order to illustrate how disorder affects the vibrational line shape. Section V contains a summary.

II. THEORY

The aim of this section is to review and elaborate on the basic theoretical frame necessary for the interpretation of the experimental data presented in Sec. III. We first discuss a very simple model for vibrational energy and phase relaxation, illustrated in Fig. 1. Here an atom (or molecule) of mass m is bonded by an anharmonic spring (e.g., a Morse potential) to the metal atom M . The crystal is assumed to be harmonic. This model has been studied in a large number of papers, both in the context of vibrational energy and phase relaxation¹¹⁻¹⁵ and also as a model for thermal desorption.^{16,17} The prevailing opinion is that this model accounts for the dominating contribution to the observed linewidth for many low-frequency adsorbate modes, e.g., for the Pt-CO stretch vibration for CO on Pt(111). However, as will be shown below, in all these treatments an important factor has been overlooked; accounting for this "missing factor" gives strongly reduced rates for vibrational energy (multiple phonon emission) and phase relaxation. Hence, we find that unless the frequency Ω of the localized mode is very close to ω_c where ω_c is the highest phonon frequency, this mechanism is unimportant.

Following Ref. 11, assume that the interaction energy between the adatom m and the metal atom M (see Fig. 1) can be described by a Morse potential

$$U(u-v) = E_0(e^{-2\alpha(u-v)} - 2e^{-\alpha(u-v)}), \quad (1)$$

where u and v are the displacements along the z direction of the adatom m and the metal atom M , respectively. E_0 is the adsorption energy and α can be related to the vi-

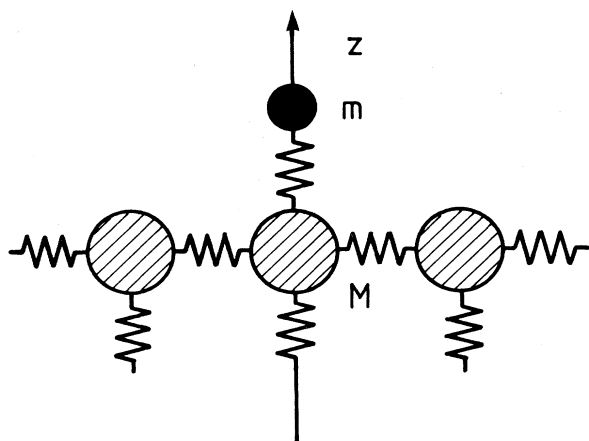


FIG. 1. A schematic picture of an adatom (or molecule) of mass m bonded via an anharmonic spring to a metal atom (mass M) on a metal surface.

brational frequency Ω of the first vibrational excited state of the localized oscillator (m vibrates against the metal atom M),

$$\alpha = (m\Omega^2/2E_0)^{1/2}. \quad (2)$$

We have implicitly assumed $m \ll M$ so that the reduced mass m^* to a good approximation equals the adsorbate mass m . Let us expand (1) in powers of $(u-v)$:

$$U = -E_0 + \frac{1}{2}m\Omega^2(v-u)^2 + E_0\alpha^3(v-u)^3 + \frac{7}{12}E_0\alpha^4(v-u)^4 + \dots \quad (3)$$

Within the harmonic approximation, the equation of motion for the adatom is

$$m \frac{d^2u}{dt^2} + m\Omega^2(u-v) = 0. \quad (4)$$

In the limit $m \ll M$ the motion of the metal atom M can be neglected, when considering the localized mode Ω , i.e., we can put $v=0$ in (4) in this case. It is easy to improve on this approximation if necessary. We now quantize the localized mode by introducing creation b^\dagger and annihilation b operators

$$u_{\text{loc}} = \left[\frac{\hbar}{2m\Omega} \right]^{1/2} (b + b^\dagger) \equiv s(b + b^\dagger).$$

Next, if the contribution from the continuum modes $q\sigma$ (wave vector q and mode index σ) to v is denoted by

$$\sum_{q\sigma} \left[\frac{\hbar}{2MN\omega_{q\sigma}} \right]^{1/2} \mathbf{e}_{q\sigma} \cdot \hat{z} (b_{q\sigma} + b_{q\sigma}^\dagger)$$

then it follows from (4) that the contribution from the continuum modes to u will be

$$\sum_{q\sigma} \frac{\Omega^2}{\Omega^2 - \omega_{q\sigma}^2} \left[\frac{\hbar}{2MN\omega_{q\sigma}} \right]^{1/2} \mathbf{e}_{q\sigma} \cdot \hat{z} (b_{q\sigma} + b_{q\sigma}^\dagger).$$

In these equations, $\mathbf{e}_{q\sigma}$ is the polarization vector. Using these equations we get

$$\begin{aligned} u-v &= \left[\frac{\hbar}{2m\Omega} \right]^{1/2} (b + b^\dagger) \\ &+ \sum_{q\sigma} \frac{\omega_{q\sigma}^2}{\Omega^2 - \omega_{q\sigma}^2} \left[\frac{\hbar}{2MN\omega_{q\sigma}} \right]^{1/2} \mathbf{e}_{q\sigma} \cdot \hat{z} (b_{q\sigma} + b_{q\sigma}^\dagger) \\ &\equiv \hat{\xi} + \hat{\eta}. \end{aligned} \quad (5)$$

This formula corrects earlier work, where the factor $\omega_{q\sigma}^2/(\Omega^2 - \omega_{q\sigma}^2)$ occurring in $\hat{\eta}$ was overlooked. But this extra factor tends to give a strong reduction in the cross section for various multiple-phonon processes such as vibrational energy and phase relaxation (see below).

For later purposes let us introduce new creation and annihilation operators B^\dagger and B so that $\hat{\eta} = S(B + B^\dagger)$, i.e.,

$$SB = \sum_{q\sigma} \frac{\omega_{q\sigma}^2}{\Omega^2 - \omega_{q\sigma}^2} \left[\frac{\hbar}{2MN\omega_{q\sigma}} \right]^{1/2} \mathbf{e}_{q\sigma} \cdot \hat{z} b_{q\sigma}.$$

The normalization factor S is chosen so that $[B, B^\dagger] = 1$, i.e.,

$$|S|^2 = \sum_{q\sigma} \left[\frac{\omega_{q\sigma}^2}{\Omega^2 - \omega_{q\sigma}^2} \right]^2 \frac{\hbar}{2MN\omega_{q\sigma}} |\mathbf{e}_{q\sigma} \cdot \hat{\mathbf{z}}|^2$$

$$= \int d\omega \rho(\omega) \left[\frac{\omega^2}{\Omega^2 - \omega^2} \right]^2 \frac{\hbar}{2M\omega}, \quad (6)$$

where the projected density of states

$$\rho(\omega) = \frac{1}{N} \sum_{q\sigma} |\mathbf{e}_{q\sigma} \cdot \hat{\mathbf{z}}|^2 \delta(\omega - \omega_{q\sigma}). \quad (7)$$

Note that ρ is normalized so that

$$\int d\omega \rho(\omega) = 1.$$

The general form of the function $\rho(\omega)$ is shown in Fig. 2. The sharp peak at ω_1 is associated with the surface-phonon modes. This peak typically carries a spectral weight (area) of $z \approx 0.7$. Since the peak in ρ is narrow and carries most of the spectral weight we can interpret B^\dagger as the creation operator for a quasilocized mode (resonance frequency ω_1 and width $\eta \approx 20 \text{ cm}^{-1}$). The physical origin of this peak is a band-edge surface phonon.

Consider now the anharmonic terms in the expansion (3) and substitute $v - u = \hat{\xi} + \hat{\eta}$ in this equation. The first two terms which to lowest order in perturbation theory give rise to the decay of the localized oscillator (via emission of 2 and 3 phonons, respectively) are

$$3E_0\alpha^3\hat{\xi}\hat{\eta}^2 + \frac{7}{3}E_0\alpha^4\hat{\xi}\hat{\eta}^3 = A\hat{\xi}\hat{\eta}^2 + B\hat{\xi}\hat{\eta}^3.$$

The leading contribution to the dephasing comes from the term

$$\frac{7}{2}E_0\alpha^4\hat{\xi}^2\hat{\eta}^2 = C\hat{\xi}^2\hat{\eta}^2$$

taken to first order in perturbation theory, and, as shown by Zhang and Langreth,¹⁵ from the term

$$A\hat{\xi}^2\hat{\eta}$$

taken to second order in perturbation theory. Thus the total Hamiltonian describing the vibrational properties of the adsorbate-metal system is taken to be

$$H = \Omega b^\dagger b + \sum_{q\sigma} \omega_{q\sigma} b_{q\sigma}^\dagger b_{q\sigma} + A(\hat{\xi}\hat{\eta}^2 + \hat{\xi}^2\hat{\eta})$$

$$+ B\hat{\xi}\hat{\eta}^3 + C\hat{\xi}^2\hat{\eta}^2. \quad (8)$$

From here on the calculation of the vibrational energy

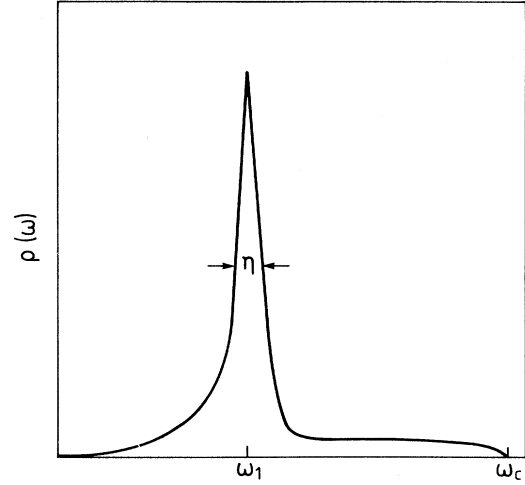


FIG. 2. The local phonon density of states at a surface atom projected on the z direction.

and phase relaxation follows earlier treatments^{11,15} and we will only give the final results.

A. Energy relaxation

(a) Assuming $\Omega < 2\omega_c$, where ω_c is the highest phonon-phonon frequency of the crystal, decay via emission of two phonons is energetically allowed and given by

$$w_2 = \frac{\Omega}{E_0} \left[\frac{m}{M} \right]^2 \Omega K_2, \quad (9)$$

where

$$K_2 = \frac{9\pi}{8} \int d\omega \rho(\omega) \rho(\Omega - \omega) [n(\omega) + n(\Omega - \omega) + 1]$$

$$\times \frac{\Omega^3}{\omega(\Omega - \omega)} \left[\frac{\omega^2}{\Omega^2 - \omega^2} \right]^2 \left[\frac{(\Omega - \omega)^2}{\Omega^2 - (\Omega - \omega)^2} \right]^2. \quad (10)$$

(b) Assuming $\Omega < 3\omega_c$ decay via emission of three phonons is energetically allowed and given by

$$w_3 = \left[\frac{\Omega}{E_0} \right]^2 \left[\frac{m}{M} \right]^3 \Omega K_3, \quad (11)$$

where

$$K_3 = \frac{49\pi}{32} \int d\omega d\omega' \rho(\omega) \rho(\omega') \rho(\Omega - \omega - \omega') \{ [n(\omega) + 1][n(\omega') + 1][n(\Omega - \omega - \omega') + 1] - n(\omega)n(\omega')n(\Omega - \omega - \omega') \}$$

$$\times \frac{\Omega^4}{\omega\omega'(\Omega - \omega - \omega')} \left[\frac{\omega^2}{\Omega^2 - \omega^2} \right]^2 \left[\frac{\omega'^2}{\Omega^2 - \omega'^2} \right]^2 \left[\frac{(\Omega - \omega - \omega')^2}{\Omega^2 - (\Omega - \omega - \omega')^2} \right]^2. \quad (12)$$

B. Phase relaxation

The leading contribution to the rate of vibrational phase relaxation comes from the terms $C\hat{\xi}^2\hat{\eta}^2$ and $A\hat{\xi}^2\hat{\eta}$ taken to first and second order in perturbation theory, respectively. The rate of phase relaxation is given by

$$\omega = \left[\frac{\Omega}{E_0} \right]^2 \left[\frac{m}{M} \right]^2 \left[\frac{\Omega}{\omega_1} \right]^3 \Omega K, \quad (13)$$

where $K = K_A + K_C$ with

$$K_C = \frac{49\pi}{32} \int d\omega \rho^2(\omega) \frac{\omega_1^3}{\omega^2} \left[\frac{\omega^2}{\Omega^2 - \omega^2} \right]^4 n(\omega)[n(\omega) + 1] \quad (14)$$

and as shown by Zhang and Langreth¹⁵

$$K_A = \frac{81}{196} K_C. \quad (15)$$

From (13) it follows that dephasing is particularly important when $\rho(\omega)$ is sharply peaked about some frequency ω_1 . If $\rho(\omega)$ is taken to be a Lorentzian with the full width at half maximum (FWHM) η , then, as shown by Zhang and Langreth,¹⁵ (14) reduces to

$$K_C = \frac{49}{32} \frac{\omega_1}{\eta} \left[\frac{\omega_1^2}{\Omega^2 - \omega_1^2} \right]^4 n(\omega_1)[n(\omega_1) + 1]. \quad (16)$$

It is obvious that (16) does not hold as $\eta \rightarrow 0$, since in this limit $K_C \rightarrow \infty$ so that lowest-order perturbation theory on which (16) is based breaks down. A very convenient and instructive way to treat the general problem of arbitrary η is as follows. Note first that

$$C\hat{\xi}^2\hat{\eta}^2 = CS^2s^2(b + b^\dagger)^2(B + B^\dagger)^2 \rightarrow 4CS^2s^2B^\dagger B b^\dagger b,$$

where we account only for the most important dephasing term. Substituting this result in the Hamiltonian (8) gives a term of the form

$$(\Omega + 4CS^2s^2B^\dagger B)b^\dagger b$$

plus other (harmonic) terms which couple the quasilocalized mode B to a continuum. Now, treating $B^\dagger B \rightarrow n(t)$ as a stochastic fluctuating variable, which can take the values $n=0, 1, 2, \dots$ leads to the problem of calculating the line shape of an oscillator with a stochastically fluctuating resonance frequency,

$$\Omega(t) = \Omega + \delta\omega n(t), \quad (17)$$

$$\delta\omega = 4CS^2s^2. \quad (18)$$

This problem has been studied in great detail elsewhere, where accurate solutions have been presented not only for a single oscillator but for the more general case of an infinite periodic system of oscillators with arbitrary lateral (e.g., dipole-dipole) interactions.¹⁸ The basic physical picture behind the dephasing process is now as follows: According to the fluctuation-dissipation theorem, an oscillator with the damping η will have an occupation $n(t)$ which fluctuates in time between $n=0, 1, 2, \dots$ in a stochastic manner determined by the damping η , the temperature T , and the excitation energy ω_1 . This will

give rise to a modulation of the resonance frequency according to (17) leading both to a frequency shift and a damping. For example, when $\eta \gg \delta\omega$ and in the absence of lateral interactions, the linewidth Γ and the frequency shift $\Delta\Omega$ can be calculated analytically:¹⁹

$$\Gamma = 2n(\omega_1)[n(\omega_1) + 1]\delta\omega^2/\eta, \quad (19)$$

$$\Delta\Omega = \delta\omega n(\omega_1), \quad (20)$$

where from (6) and (18)

$$\delta\omega = \frac{7}{8} \frac{\Omega}{E_0} \frac{m}{M} \frac{\Omega}{\omega_1} \left[\frac{\omega_1^2}{\Omega^2 - \omega_1^2} \right]^2 \Omega.$$

Substituting this in (19) gives, as expected, the same result as presented before [Eqs. (14) and (16)]. In general, however, no simple analytical result exists for the line profile which therefore must be calculated numerically from the equations given in Ref. 18.

Let us now estimate the magnitude of the rate of energy and phase relaxation for the Pt-CO stretch vibration due to the direct coupling to the crystal. Using $\Omega = 460 \text{ cm}^{-1}$, $E_0 = 1.3 \text{ eV}$, and $\omega_1 = 70 \text{ cm}^{-1}$ gives $\delta\omega = 0.01 \text{ cm}^{-1}$. Since the width η of the quasilocalized phonon is about 20 cm^{-1} from Eq. (20) we calculate the dephasing contribution at room temperature to be $\Gamma \approx 10^{-4} \text{ cm}^{-1}$. This is about a factor 10^{-4} times smaller than observed experimentally. Note that the small magnitude of $\delta\omega$ and Γ is due to the "missing factor" which reduces $\delta\omega$ by a factor $\sim 5 \times 10^{-4}$ and Γ by a factor $\sim 2.5 \times 10^{-7}$. Similarly the contribution to the linewidth from decay via emission of three bulk phonons (decay via emission of two bulk phonons is energetically forbidden) is extremely small. For example, using (12) and (13) and assuming a Debye density of phonon states (which overestimates the decay rate) gives at room temperature $\Gamma = 2 \times 10^{-5} \text{ cm}^{-1}$.

In the discussion above we have considered energy and phase relaxation due to the direct coupling to the substrate phonons. The dephasing process can be considered as resulting from the anharmonic coupling to a quasilocalized surface phonon. But both the energy and phase relaxation processes were found to be extremely weak and cannot explain the experimental data to be presented in Sec. III. We will now demonstrate that there exists another dephasing process, which for CO on Pt(111) is much more important. In a recent work Lahee *et al.*⁸ have shown that CO in the on-top position on Pt(111) has a parallel frustrated translation with a very low frequency, $\omega_T \approx 50\text{--}60 \text{ cm}^{-1}$ and with a damping less than $\sim 20 \text{ cm}^{-1}$. This mode is coupled anharmonically to the Pt-CO stretch vibration Ω . If we consider Ω to depend parametrically on the normal mode coordinate Q of the frustrated translation, then by symmetry Ω is unchanged as $Q \rightarrow -Q$ and to lowest nonvanishing order in Q

$$\Omega(Q) \approx \Omega(0) + aQ^2. \quad (21)$$

Note that the a parameter can be related to the change $\delta\omega$ in the Pt-CO stretch frequency as this mode is excited from its n th to its $(n+1)$ th state

$$a = m\omega_T\delta\omega. \quad (22)$$

One can get a rough estimate of a as follows. Assume that Ω is proportional to the square root of the Pt-CO binding energy, $\Omega \sim (E_0)^{1/2}$, as is the case for the Morse potential (1). Since

$$E_0(Q) \approx E_0(0) - m\omega_T^2 Q^2/2$$

we get

$$\Omega(Q) \approx \Omega(0)(1 - m\omega_T^2 Q^2/4E_0).$$

Hence,

$$a = -m\omega_T^2 \Omega(0)/4E_0$$

and from (22)

$$\delta\omega = -\omega_T \Omega/4E_0. \quad (23a)$$

The parameter $\delta\omega$ can also be estimated as follows. As a CO molecule is displaced from an on-top site to a bridge site, the Pt-CO frequency changes from²⁰ 470 to 380 cm^{-1} , i.e., by $\Delta\Omega = -90 \text{ cm}^{-1}$; if the expansion (21) is assumed to hold for such a large displacement we get $a = \Delta\Omega/Q_0^2$ where $Q_0 = 1.4 \text{ \AA}$ is the separation between the on-top and bridge sites. Hence using (22) gives

$$\delta\omega = \Delta\Omega/m\omega_T Q_0^2. \quad (23b)$$

For the Pt-CO stretch vibration for on-top bonded CO on Pt(111), $\Omega = 470 \text{ cm}^{-1}$. The CO binding energy is²¹ $E_0 = 1.4 \text{ eV}$ and the frequency of the parallel frustrated translation⁸ $\omega_T = 6 \text{ meV}$, so from (23a) $\delta\omega \approx -0.5 \text{ cm}^{-1}$. If we instead use (23b) we get $\delta\omega \approx -1.0 \text{ cm}^{-1}$. This anharmonic coupling parameter is much larger than that estimated for coupling to the quasilocalized surface phonon, where $\delta\omega \approx 0.01 \text{ cm}^{-1}$. This fact together with the somewhat smaller damping and lower resonance frequency for the parallel frustrated translation leads to a much larger contribution to the dephasing of the Pt-CO vibration from this mode. In fact, using (19) we estimate for room temperature $\Gamma \sim 1 \text{ cm}^{-1}$ from coupling to the frustrated translation to be compared with $\Gamma \approx 10^{-4} \text{ cm}^{-1}$ found earlier from coupling to the quasilocalized phonon. A detailed comparison between theory and experiment is given in Sec. IV.

For practical reasons the IRS studies of adsorbate vibrations are not performed on isolated molecules but rather on surfaces with a finite concentration of adsorbates. Hence one must in general account for the interaction between the adsorbates. For the Pt-CO stretch vibration the dynamical dipole-dipole coupling is extremely weak and can be neglected. However, for coverages between those where ordered adsorbate structures prevail, the system will be disordered. Due to the unbalanced forces acting between the CO molecules in disordered adsorbate systems, the molecules will be displaced away from the substrate symmetry points. This will lead to a distribution of Pt-CO stretch frequencies which will broaden and shift the infrared absorption peaks. The contribution to the line shift and width from this process is easily estimated using the model presented above, if we assume that the Pt-CO stretch frequency of the i th CO molecule can be written as

$$\Omega \approx \Omega_0 + aQ_i^2.$$

Here we have implicitly assumed that the frequency depends mainly on the displacement Q_i away from the symmetry site and not on the direct or indirect (via the metal substrate) chemical interaction between the CO molecules. The total (or average) polarizability of the system is then proportional to

$$\frac{1}{N} \sum_i \frac{1}{\omega - \Omega_0 - aQ_i^2 - i\Gamma_0} = \left\langle \frac{1}{\omega - \Omega_0 - aQ^2 - i\Gamma_0} \right\rangle,$$

where N now denotes the total number of adsorbed molecules. This expression can also be written as

$$\frac{1}{2\pi} \int d\omega' \frac{1}{\omega - \omega' - \Omega_0 - i\Gamma_0} \int dt \langle e^{i(\omega' - aQ^2)t} \rangle. \quad (24)$$

Using the cumulant expansion to second order we get

$$\langle e^{-iaQ^2 t} \rangle = e^{-ia\langle Q^2 \rangle t - a^2(\langle Q^4 \rangle - \langle Q^2 \rangle^2)t^2/2}.$$

The t integral is now easy to evaluate giving (in the limit $\Gamma_0 \rightarrow 0$) a Gaussian line shape with the FWHM and frequency shift

$$\Gamma = m\Omega_0 |\delta\omega| [8 \ln(2)(\langle Q^4 \rangle - \langle Q^2 \rangle^2)]^{1/2}, \quad (25)$$

$$\Delta\Omega = m\Omega_0 \delta\omega \langle Q^2 \rangle. \quad (26)$$

In Sec. IV we perform Monte Carlo simulations in order to study the effect of disorder on the Pt-CO vibrational line profile and Eqs. (25) and (26) will then be used to estimate the contribution to the linewidth and frequency shift.

Disorder in an adsorbate system may also result from the irregular thermal motion occurring at nonzero temperatures. For example, for the $c(4 \times 2)$ system the most low-energetic nonvibrational excitation corresponds to a CO molecule jumping from a bridge site to a displaced on-top site, as has been discussed in detail elsewhere.⁹ Due to the unbalanced repulsive CO-CO interactions, the CO molecules in the vicinity of such an excitation will be displaced away from the substrate symmetry sites. This "thermal disorder" may broaden the Pt-CO vibrational peak. Furthermore, at high enough temperature the system may exhibit an order-disorder transition which could result in a strong increase in the linewidth. These effects have been studied for the internal C-O vibration in an earlier paper,⁹ and in Sec. IV we will study the same effect for the Pt-CO mode. We note here that if the nonvibrational excitations have a long lifetime, as in the present case (resulting from activation barriers of order ~ 0.2 – 0.3 eV) then the thermal disorder changes slowly in time and is mathematically equivalent to static disorder. Nevertheless, strictly speaking, for a system in thermal equilibrium these processes are normal phase relaxation.

III. EXPERIMENTAL

The investigated system is CO chemisorbed on a Pt(111) surface. The experimental conditions will be described elsewhere.²² In brief, the crystal was oriented

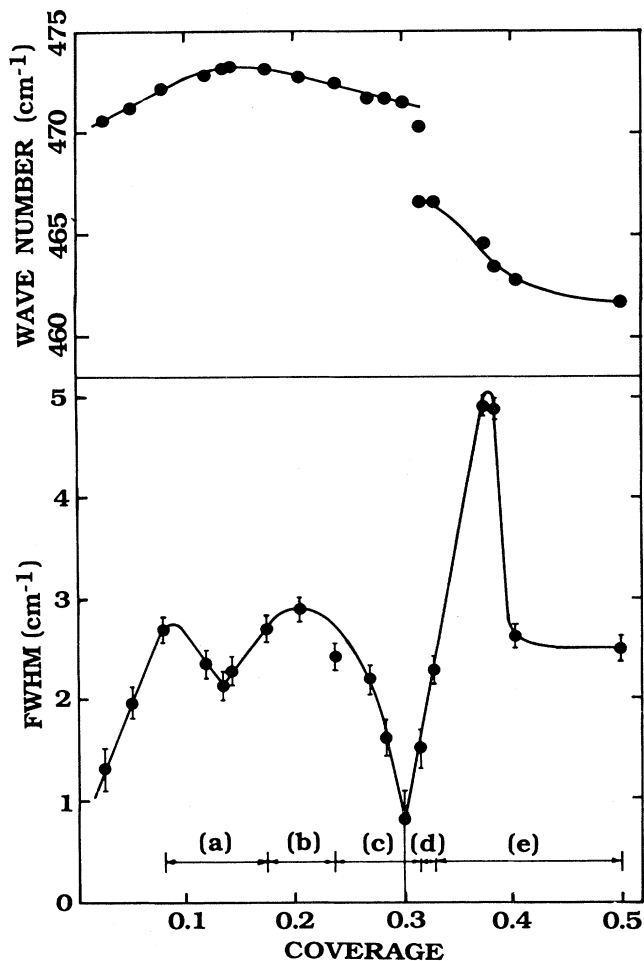


FIG. 3. The width (FWHM) and position of the infrared absorption peak of the on-top bonded molecules of CO on Pt(111) as function of coverage. The spectra are taken at 100 K and the spectrometer band pass of 2.6 cm^{-1} is subtracted. Indicated is also the observed LEED pattern as (a) (4×4) , (b) diffuse $(\sqrt{3} \times \sqrt{3})R30^\circ$, (c) (8×8) , (d) $(8 \times 8) + c(4 \times 2)$, and (e) $c(4 \times 2)$.

within 0.3° and mechanically polished. The *in situ* cleaning consisted of numerous cycles of annealing in vacuum at 1150 K, oxidation (10^{-6} torr O_2) at 1000 K and low-energy sputtering (Ar^+ , 250 eV, $1 \mu A/cm^2$) at room temperature. During these procedures the surface kept its mirrorlike finish. The infrared spectra were recorded with a dispersive vacuum spectrometer using the wavelength modulation technique. Consecutive difference spectra were constructed and integrated, as previously described. The CO depositions were made at 250 K and after cooling the spectra were recorded at 100 K, if not stated otherwise.

Figure 3 shows the full width at half maximum and position of the infrared absorption peak of the Pt-CO stretch vibrational mode for the on-top bonded molecules

as a function of coverage at 100 K. The spectrometer resolution of 2.6 cm^{-1} is subtracted, assuming Gaussian distributions (that the widths add quadratically). Doses have been converted to coverage using the sticking coefficient reported by Steininger *et al.*²⁰ [assuming $\Theta = 0.3$ for the (8×8) structure]. The surprisingly strong and sharp variation of the width with coverage indicates that the width is dominated by inhomogeneous broadening caused by structural disorder in the overlayer, as the effect of surface defects and contamination as well as vibrational damping and dephasing are expected to be rather independent of the CO coverage. Such a strong coverage dependence of the width, as indicated in Fig. 3, has not been previously reported. The main reason is that a vibrational mode that is so sensitive to structural disorder is equally sensitive to other kinds of inhomogeneities, which may then dominate and mask the effect, as in the previously reported work.⁵⁻⁷

The CO/Pt(111) system exhibits three ordered, uncompressed, structures at low temperatures.²⁰ The $c(4 \times 2)$ structure corresponds to a coverage (with respect to the number of Pt atoms) $\Theta = 0.5$, with half of the molecules in on-top position and half of them bridge bonded. For the two low-coverage structures Tüshaus *et al.*²³ have proposed real-space models, denoted (4×4) and (8×8) , with all molecules in on-top position and $\Theta = 0.19$ and 0.30 , respectively. In Fig. 3 the sequence of observed low-energy electron diffraction patterns (LEED) is indicated and from this it is obvious that the minima in the width are connected with the ordering in the overlayer. Starting with the (8×8) structure at $\Theta = 0.30$, the data show a very sharp order-disorder transition. The width for the ordered structure is below 1 cm^{-1} , accompanied with a sharp (8×8) LEED pattern. The ordering of the (4×4) structure has the same discontinuous character, but shows a pretty large residual inhomogeneous width. This indicates that it is not possible to obtain a well-ordered (4×4) structure, which is confirmed by the LEED pattern showing rather diffuse spots.

When the coverage is increased above $\Theta = 0.3$, a good $c(4 \times 2)$ LEED pattern develops already at $\Theta = 0.33$. The overlayer must turn into a very disordered state, with $c(4 \times 2)$ islands in a disordered matrix. This is seen in the very large increase of the peak width, which then gradually decreases when the overlayer develops a more and more homogeneous $c(4 \times 2)$ structure. The transition has of course a continuous character.

The $(8 \times 8) - c(4 \times 2)$ transition is also seen in the peak position in Fig. 3. The coexistence of two peaks at $\Theta = 0.32$ shows that there is no continuous transition of the vibrational frequency, but that the two different modes belong to two different situations. The mode with the vibration frequency above 470 cm^{-1} is associated with molecules having only on-top bonded neighbors, while the mode around 465 cm^{-1} is connected to the on-top bonded molecules in or close to a $c(4 \times 2)$ island.

Figure 4 shows the peak width and position as a function of substrate temperature for the $c(4 \times 2)$ structure. We observe two temperature-dependent contributions to the width, one operating over the whole measured temperature range and one setting in at 250 K.

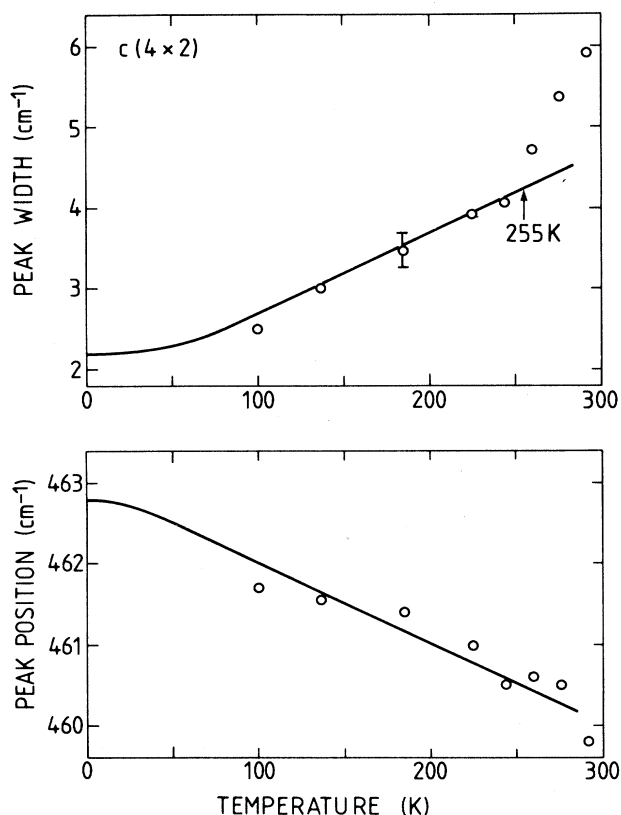


FIG. 4. The width (FWHM) and position of the infrared absorption peak for on-top bonded CO on Pt(111) in the $c(4 \times 2)$ structure. The solid lines are theoretical results discussed in the text.

IV. ANALYSIS OF THE EXPERIMENTAL DATA

We focus first on the temperature dependence of the linewidth for the $c(4 \times 2)$ structure shown in Fig. 4. The solid lines in the figure are theoretical results¹⁸ based on vibrational dephasing via anharmonic coupling to the frustrated translation, as discussed above. In the calculation we have used (in cm^{-1})

$$\omega_0 = 60, \quad \delta\omega = -1.2, \quad \text{and} \quad \eta = 6.$$

The resonance frequency $\omega_0 = 60 \text{ cm}^{-1}$ of the frustrated translation is in accordance with earlier inelastic helium scattering results,⁸ and the anharmonicity parameter $\delta\omega = -1.2 \text{ cm}^{-1}$ is close to the two estimates presented in Sec. III. The damping $\eta = 6 \text{ cm}^{-1}$ is slightly smaller than the $\eta = 10 \text{ cm}^{-1}$ used in Ref. 9 in the analysis of the dephasing contribution to the linewidth of the internal C-O stretch vibration. However, as was pointed out in that work, the influence of the damping on the linewidth for the C-O stretch vibration is negligible as long as the

damping is smaller than the bandwidth associated with the dipole-dipole coupling and an equally good fit to that experimental data is obtained using, e.g., $\eta = 5 \text{ cm}^{-1}$. The theoretical estimate of η using the elastic continuum model,¹⁹

$$\eta = \frac{3}{8\pi} \frac{m}{\rho} \left[\frac{\omega_0}{c_T} \right]^3 \omega_0 \quad (27)$$

with $\rho = 2140 \text{ kg/m}^3$, $c_T = 1600 \text{ m/s}$, and $\omega_0 = 60 \text{ cm}^{-1}$ gives $\eta = 5 \text{ cm}^{-1}$. (The theoretical value $\eta = 10 \text{ cm}^{-1}$ quoted in Ref. 9 is in error.)

At very low temperature the effect of the phase relaxation vanishes, as the frustrated translation is no longer excited. We are then left with a temperature-independent contribution to the width of about 2 cm^{-1} . In the work on the internal C-O mode this contribution was about 5 cm^{-1} and was associated with the homogeneous broadening due to vibrational damping. However, as mentioned above we have shown elsewhere that for the Pt-CO mode the homogeneous broadening is less than 1 cm^{-1} , so this constant contribution must be caused by a temperature-independent inhomogeneous broadening due to structural disorder.

As discussed elsewhere,²² the temperature dependence for the (8×8) structure is completely dominated by an order-disorder transition.

Let us now consider the coverage dependence of the linewidth Γ . As discussed in Sec. II, a source of inhomogeneous broadening arises from the displacements Q_i of the CO molecules away from the substrate symmetry points, which occur in disordered adsorbate systems due to the unbalanced CO-CO interactions. The contribution to the linewidth from this "disorder" can be estimated using Eq. (25) with $\langle Q^2 \rangle$ and $\langle Q^4 \rangle$ obtained from Monte Carlo simulations. But accurate MC simulations require as an input an accurate CO-Pt potential energy surface as well as a knowledge about the effective CO-CO interaction potential for adsorbed CO molecules. Based on experimental information, these two quantities were constructed in an earlier paper⁹ and for the details the reader is referred to this paper. Here we only note that this MC study is in relative good agreement with experiment. For example, as a function of temperature the $c(4 \times 2)$ structure was found to exhibit an order-disorder transition at $T_c \approx 260 \text{ K}$ which is very close to the transition temperature, $T_c(\text{expt.}) \approx 275 \text{ K}$. Furthermore, the $c(4 \times 2)$ structure as well as all the compressed structures for $\Theta > 0.5$ were reproduced. However, for $\Theta < 0.5$ only one ordered structure was obtained, namely the triangular $(\sqrt{3} \times \sqrt{3})R30^\circ$ structure. Both of the suggested²³ (4×4) and (8×8) structures are built up from patches of the $(\sqrt{3} \times \sqrt{3})R30^\circ$ units separated by low-density antiphase boundaries with (4×4) and (8×8) periodicity.

We will now use MC calculations to illustrate in a semiquantitative way the influence of disorder on the vibrational spectra. Following Ref. 10 the calculations were performed using periodic boundary conditions, with the basic unit cell taken as an $M \times M$ rectangle, where the number of Pt atoms M in the x and y directions was varied ($M = 6$ or 12). Initially all the CO molecules were

placed in on-top position on one side of the basic unit. After $\sim 100\,000$ Monte Carlo steps per particle the system reached thermal equilibrium after which the quantities $\langle Q^2 \rangle$ and $(\langle Q^4 \rangle - \langle Q^2 \rangle^2)^{1/2}$ was calculated by averaging over all the CO molecules in the basic unit and over many ($\sim 100\,000$ MC steps per particle) extra MC steps.

Figure 5 shows the adsorbate system ($M=6$) for a few

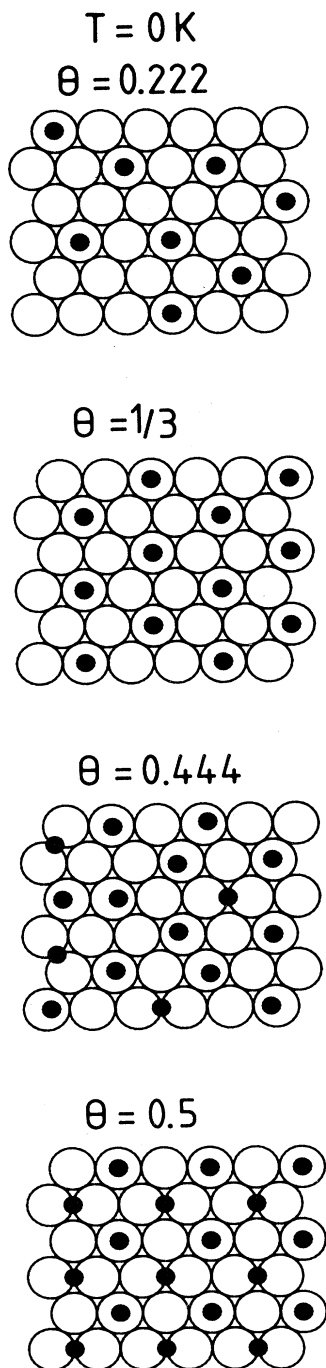


FIG. 5. A sequence of Monte Carlo pictures of the adsorbate system at different coverages and at zero temperature.

different coverages and at zero temperature. The MC results were obtained by cooling the system very slowly from $T=500$ to 0 K. Note that at low coverages the CO molecules sit at the symmetry points of the substrate while at high CO coverages they are displaced away from these points by the unbalanced CO-CO repulsions. This is illustrated in more detail in Fig. 6, which shows $\langle Q^2 \rangle$ and $(\langle Q^4 \rangle - \langle Q^2 \rangle^2)^{1/2}$ in units of R^2 (where $R \approx 1.4$ Å is the radius of a Pt atom). Results are shown for $T=0$ and 100 K. Note that to within the accuracy of the numerical simulation, $\langle Q^2 \rangle$ and $\langle Q^4 \rangle$ evaluated at $T=100$ K is the sum of the contribution from the configurational disorder alone ($T=0$ K curves) plus a smooth (as a function of coverage) background contribution (dashed lines) arising from the parallel vibrational motion in the local potential wells in the disordered system. Note that this latter contribution decreases with increasing coverage because of the repulsive CO-CO interaction, which stiffens the frequencies for the parallel frustrated translations as the coverage increases (from 49 cm^{-1} at low coverage to 60

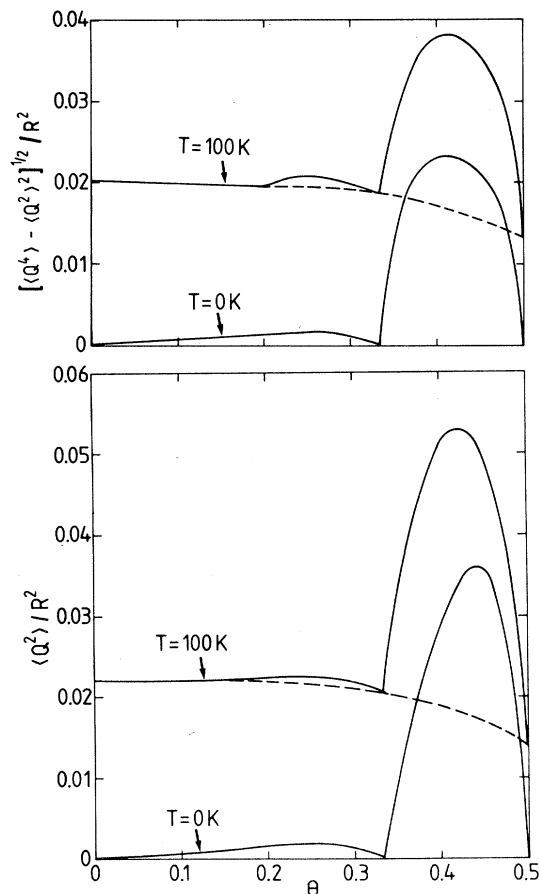


FIG. 6. (a) The average of the square of the displacement of the on-top bonded CO molecules away from the substrate symmetry points as obtained from the Monte Carlo simulations. The result for $\langle Q^2 \rangle$ at $T=100$ K is approximately the sum of $\langle Q^2 \rangle$ at $T=0$ K plus the contribution from the parallel CO vibrational motion. (b) The rms deviation of the square of the displacement of the on-top bonded CO molecules away from the substrate symmetry points. The unit of length $R = 1.4$ Å is the radius of a Pt-atom.

cm^{-1} at $\Theta=0.5$).⁸ When studying the disorder contribution to the linewidth the vibrational contribution should be excluded, i.e., we use the $T=0$ K results for $\langle Q^2 \rangle$ and $\langle Q^4 \rangle$. In fact the contribution to the linewidth from the vibrational motion cannot be accounted for by using (26) since this equation is valid only when the disorder changes slowly in time giving rise to essentially static disorder. Instead the contribution from the vibrational motion must be calculated separately by using the full line-shape theory⁹ as discussed above for the temperature-dependent contribution to the linewidth for (4×2) structure.

Using (25) and Fig. 6 we can estimate the contribution to the linewidth from disorder. Since $m\Omega_0|\delta\omega|R^2 \approx 110 \text{ cm}^{-1}$, the disorder-induced contribution to the linewidth for $0.33 < \Theta < 0.5$ is about 5 cm^{-1} , in good agreement with the maximum linewidth occurring between the (8×8) and $c(4 \times 2)$ structures shown in Fig. 3. For $\Theta < 0.33$ negligible disorder-induced contribution to the linewidth occurs in the calculation—the reason for this is, of course, that the average nearest-neighbor distance between the CO molecules in this case is relatively “large” so that only very small displacements of the CO molecules away from the substrate symmetry points occur as a result of the short-ranged repulsive CO-CO interactions. The experimental data still exhibit some disorder-induced line broadening for $\Theta < 0.3$ which we suggest to be caused by the long-ranged tail of the indirect CO-CO interaction^{24,25} (not included in our model calculation).

V. SUMMARY

This work has considered the properties of the metal-molecule stretch vibrational mode of adsorbed molecules, in particular CO chemisorbed on a Pt(111) surface. We have shown that there is a missing factor in the previously published theories on the vibrational coupling between this mode and the metal phonons, which decreases the strength of the interaction with several orders of magnitude.

The experimental results show that the infrared spectra of this mode are very sensitive to inhomogeneous broadening and that this sensitivity can be used to study the ordering in the overlayer. The temperature dependence of the peak shape is very well explained by the anharmonic coupling to the frustrated translation, just as for the high-frequency C-O stretch mode. The parameter values used in the calculation are obtained from independent experiments or could be rather accurately estimated. Hence, this definitely shows that this theory gives a good description of the dephasing process and the obtained parameter values are related to relevant physical properties.

Using Monte Carlo simulations of the ordering in the overlayer, we are also able to get a deeper insight in the coverage-dependent inhomogeneous broadening, as they are seen in the experimental data. We show that the broadening has two components, a disorder-induced contribution plus (at temperatures above 50 K), a contribution from the thermally excited frustrated translation.

¹F. M. Hoffmann, *Surf. Sci. Rep.* **3**, 107 (1983).

²A. M. Bradshaw and E. Schweizer, in *Advances in Spectroscopy*, edited by R. E. Hester (Wiley, New York, 1988).

³Y. J. Chabal, *Surf. Sci. Rep.* **8**, 211 (1988).

⁴R. Ryberg, in *Advances in Chemical Physics, Molecule Surface Interactions*, edited by K. P. Lawley (Wiley, London, 1989).

⁵R. G. Tobin and P. L. Richards, *Surf. Sci.* **179**, 387 (1987).

⁶D. Hoge, M. Tushaus, E. Schweizer, and A. M. Bradshaw, *Chem. Phys. Lett.* **151** 230 (1988).

⁷I. J. Malik and M. Trenary, *Surf. Sci.* **214**, L237 (1989).

⁸A. M. Lahee, J. P. Toennies, and Ch. Woll, *Surf. Sci.* **177**, 371 (1986).

⁹E. Schweizer, B. N. J. Persson, M. Tushaus, and A. M. Bradshaw, *Surf. Sci.* **213**, 49 (1989).

¹⁰B. N. J. Persson, *Phys. Rev. B* **40**, 7115 (1989).

¹¹B. N. J. Persson, *J. Phys. C* **17**, 4741 (1984).

¹²J. C. Ariyasu, D. L. Mills, K. G. Lloyd, and J. C. Hemminger, *Phys. Rev. B* **30**, 507 (1984).

¹³A. I. Volokitin, O. M. Braun, and V. M. Yakovlev, *Surf. Sci.* **172**, 31 (1986).

¹⁴M. Hutchinson and T. F. George, *Chem. Phys. Lett.* **124**, 211 (1986).

¹⁵Z. Y. Zhang and D. C. Langreth, *Phys. Rev. Lett.* **59**, 2211

(1987).

¹⁶C. Jedrzejek, K. F. Freed, S. Efrima, and H. Metiu, *Chem. Phys. Lett.* **74**, 43 (1980); S. Efrima, C. Jedrzejek, K. F. Freed, E. Hood, and H. Metiu, *J. Chem. Phys.* **79**, 2436 (1983).

¹⁷A. Nitzan and B. Carmeli, *Isr. J. Chem.* **22**, 360 (1982). The approximations invoked in this work result in zero-energy relaxation rate.

¹⁸B. N. J. Persson, F. M. Hoffmann, and R. Ryberg *Phys. Rev. B* **34**, 2266 (1986).

¹⁹B. N. J. Persson and R. Ryberg, *Phys. Rev. B* **32**, 3586 (1985).

²⁰H. Steininger, S. Lewald, and H. Ibach, *Surf. Sci.* **123**, 264 (1982).

²¹G. Ertl, M. Neumann, and K. M. Streit, *Surf. Sci.* **64**, 393 (1977).

²²R. Ryberg (unpublished).

²³M. Tushaus, E. Schweizer, P. Hollins, and A. M. Bradshaw, in *Vibrations at Surfaces*, edited by A. M. Bradshaw and H. Conrad (Elsevier, Amsterdam, 1987).

²⁴T. B. Grimley, *Proc. Phys. Soc.* **90**, 751 (1967).

²⁵T. L. Einstein and J. R. Schrieffer, *Phys. Rev. B* **7**, 3629 (1973).